2023 International Symposium on Nonlinear Theory and Its Applications
NOLTA2023, September 26-29, 2023, Catania and Online

Traveling Mixed-Mode Oscillations in Resistively-Coupled Bonhoeffer-Van der Pol Oscillators

Naoki Matsumiya†, Kuniyasu Shimizu†, Naohiko Inaba‡

†Dept. of Information and Communication Systems Engineering, Chiba Institute of Technology,
2–17–1 Tsudanuma, Narashino, Chiba 275-0016, Japan
‡Graduate School of Electrical and Information Engineering, Shonan Institute of Technology,
1-1-25 Tsujidou-Nishikaigan, Fujisawa, Kanagawa 251-8501, Japan

Email: s18a5120kr@s.chibakoudai.jp, kuniyasu.shimizu@it-chiba.ac.jp

Abstract— In this study, we investigate a resistively-coupled Bonhoeffer-Van der Pol (BVP) oscillators. We explore complex mixed-mode oscillations (MMOs) in BVP oscillators subjected to periodic perturbations, which exhibit unique waveforms characterized by large amplitude excursions and small peaks. Focusing on traveling MMO-sequences in resistively-coupled BVP oscillators, we analyze the increments of large amplitude excursions using the angular frequency of the external force as a control parameter. Furthermore, we show that MMO-sequences propagate spatially in a unidirectional manner.

1. Introduction

The transmission of information between neurons relies on the propagation of electrical signals in nerve fibers. In order to replicate the axon membrane potential, the Bonhoeffer-Van der Pol (BVP) oscillator is proposed as a simplified version of the Hodgkin-Huxley model [1, 2]. This oscillator consists of two variables that correspond to the membrane potential and ionic current in the nerve segment. The nonlinearity of the ionic current gives rise to a wide variety of oscillatory phenomena.

MMOs are observed in chemical experiments and display unique waveforms in the time series [3–9], characterized by L large amplitude excursions and s small peaks, represented by the symbol L^s. In our previous works, we reported the presence of complex mixed-mode oscillations (MMOs) in BVP oscillators subjected to periodic perturbations, which were detected in both numerical and experimental results [3, 4]. Recently, we discovered that traveling MMO-sequences emerged in multi-compartment models of BVP oscillators through numerical simulations [10].

In this study, we focus on the traveling MMO-sequence observed in resistively-coupled BVP oscillators. In particular, we investigate the increments of large amplitude excursions of MMOs when we employ the anugular freuqency of the external force as a control parameter which is injected to the single edge of the coupled BVP oscillators. Furthermore, we show that MMO-sequences travel spatially in a unidirectional manner.

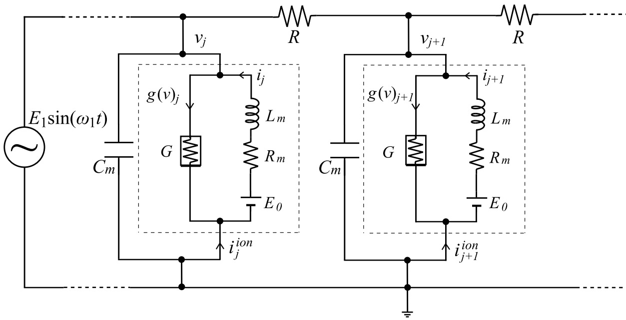

Figure 1: Resistively-coupled BVP oscillators.

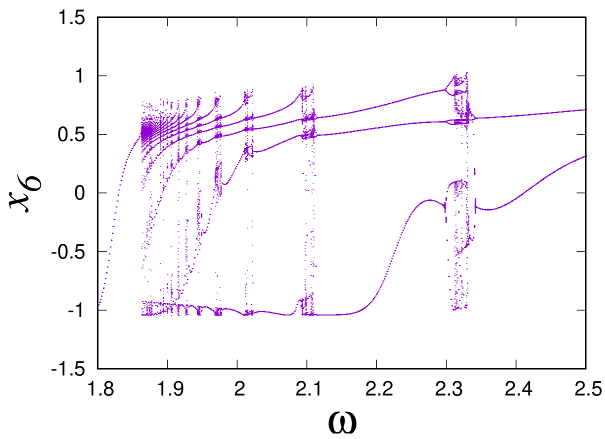

Figure 2: One-parameter bifurcation diagram in terms of ω for x_6.

2. Circuit setup

This study examines a multi-compartment model based on BVP oscillator, which includes an inductor, a capacitor, a resistor, a nonlinear conductance, and a DC voltage source. The voltage across the capacitor represents

ORCID iDs Naoki Matsumiya: 0000-0002-1385-5871, Kuniyasu Shimizu: 0000-0003-1983-2360, Naohiko Inaba: 0000-0003-1153-7025

the membrane potential, and the voltage-current characteristic of the conductance is assumed to be given by $g(v_j) = -g_1 v_j + g_3 v_j^3$, where g_1 and g_3 are positive constants. The ionic current in the membrane is represented by $i_j^{ion} = i_j - g(v_j)$. In this study, we use a multi-compartment model of BVP oscillators to simulate a cylindrical axonal nerve membrane as shown in Fig. 1. The nerve is discretized into segments of length Δx and the axoplasmic resistance between the segments depends on the resistivity ρ_j of the nodes. In this study, we assume 101 segments. The membrane potential at the single edge of the fiber is perturbed by a sinusoidal input $E_1 \sin(\omega_1 t)$. We use the zero-flux boundary condition for the membrane potential at the ends of the nerve fiber.

By using the following new parameters and the variables as

$$\varepsilon \equiv \frac{C_m}{g_1^2 L_m}, \quad k_1 \equiv g_1 R_m, \quad \sigma \equiv \frac{r}{2\rho_j g_1 (\Delta x)^2}, \quad a \equiv \frac{l}{10^{-2}},$$

$$B_0 \equiv \sqrt{\frac{g_3}{g_1}} E_0, \quad B_1 \equiv \sqrt{\frac{g_3}{g_1}} E_1, \quad \omega \equiv L_m g_1 \omega_1,$$

$$\tau \equiv \frac{t}{L_m g_1}, \quad x_j \equiv \sqrt{\frac{g_3}{g_1}} v_j, \quad y_j \equiv \sqrt{\frac{g_3}{g_1^3}} i_j,$$

the normalized membrane potential (x_j) of the multi-compartment model can be written as follows [10]

$$\varepsilon \frac{dx_j}{d\tau} = \begin{cases} \sigma_j\,(x_{j+1} - x_j) - y_j + x_j - x_j^3 \quad (j = 2) \\ \sigma_j\,(x_{j-1} - x_j) - y_j + x_j - x_j^3 \quad (j = M-1) \\ \sigma_j\,(x_{j+1} - 2x_j + x_{j-1}) - y_j + x_j - x_j^3 \\ \qquad\qquad\qquad (j = 3, \dots, M-2) \end{cases} \tag{1}$$

,where the dynamics of the normalized current (y_j) is written by

$$\frac{dy_j}{d\tau} = \begin{cases} -x_j - k_1 y_j + B_0 + B_1 \sin(\omega\tau) \quad (j = 2) \\ -x_j - k_1 y_j + B_0 \quad (j = 3, \dots, M-1). \end{cases} \tag{2}$$

The parameter k_1 plays a crucial role in determining the bifurcation structure around the equilibrium point for the isolated BVP oscillator without any periodic forcing term, as reported in [3]. Specifically, when $0 < k_1 \ll 1$, a supercritical pitch-fork bifurcation is observed as a function of B_0, while a subcritical pitch-fork bifurcation occurs with increasing k_1. In the latter case, a stable equilibrium point and a limit cycle coexist within a certain range of B_0 values. In our previous works [3,4], we reported that the coexisting region of these two solutions can exhibit complicated MMOs under the influence of a weak periodic perturbation. The degree of coupling strength between the oscillators is determined by the parameter σ_j.

3. Consecutive increments of large amplitude excursions

In this section, we explore the influence of the angular frequency of the external force ω on MMOs-sequence. Throughout this study, we fix the remaining parameters as $B_0 = 0.22$, $B_1 = 0.16$, and $k_1 = 0.9$. Furthermore, we posit that the coupling strength exhibits uniformity among the coupled BVP oscillators, with $\sigma_j = \sigma = 0.625$. In this study, we performe all numerical integrations using the initial conditions $x_j(0) = \hat{x}$ and $y_j(0) = \hat{y}$, where the initial value set $(\hat{x}, \hat{y})$ corresponds to the equilibrium point of an isolated BVP oscillator in the absence of any periodic forcing term, yielding $(\hat{x}, \hat{y}) = (0.5662, -0.3847)$.

In the subsequent results, our focus is on MMO-sequences associated with periodic oscillations. To investigate periodicity of the objective solution, we compute the Poincaré mapped points at a constant time interval of $2n\pi/\omega$, where n is a natural number. To exclude the transient, we utilize the mapped points for $100 \leq n \leq 300$. Figure 2 presents a one-parameter bifurcation diagram in which the values of x_6 at $2n\pi/\omega$ are plotted. From the diagram, it is evident that the period of the trajectory progressively increases as ω decreases.

The number of periods represents the sum of both small- and large-amplitude excursions. In particular, an increase in the period in Fig. 2 corresponds to an expansion of the large excursion. Figure 3 displays the time series of x_6 for five distinct values of ω, where periodic solutions emerge. For $\omega = 2.5$, the waveform is consistent with the periodic MMO-sequence 1^1, as illustrated in Fig. 3 (a). Whereas, for $\omega = 2.2$, the solution's period shifts to three, corresponding to the periodic MMO-sequence 2^1, as depicted in Fig. 3 (b). Likewise, it is noted that successive increases in large-amplitude excursions occur as ω declines. Moreover, the MMO-sequences propagate spatially in a unidirectional manner. Figure 4 presents a 3D plot of the time series of x_j ($j = 1, 2, \dots, M$) for $\omega = 0.205$. Figure 5 provides a magnified view of Fig. 2. From this figure, it becomes evident that large-amplitude excursions occur repeatedly as a function of ω. Figure 6 shows the time series for $\omega = 1.87$ where the waveform 24^1 is observed. Additionally, the region of existence becomes increasingly narrow with decreasing values of ω. When the value of ω is small, the limit cycle appears.

4. Conclusions

In this study, we investigated the influence of the angular frequency of the external force ω on MMO-sequences in coupled BVP oscillators. By calculating the one-parameter bifurcation diagram and investigating the time series for various values of ω, we reported that the period of the trajectory progressively increased as ω decreased, with a corresponding expansion in large-amplitude excursions. Additionally, we observed that MMO-sequences traveled spatially in a unidirectional manner.

References

[1] F. Rattay and M. Aberham, “Modeling axon membranes for functional electrical stimulation,” IEEE Trans. Biomed. Eng. vol.40, no.12, pp.1201–1209, 1993.

[2] F. Rattay and T. Tanzer, “A simple model considering spiking probability during extracellular axon stimulation,” PLOS ONE, vol.17, no.4, 2022.

[3] K. Shimizu, M. Sekikawa, N. Inaba, “Mixed-mode oscillations and chaos from a simple second-order oscillator under weak periodic perturbation,” Phys. Lett. A, vol.375, no.14, pp.1566-1569, 2011.

[4] K. Shimizu, M. Sekikawa, N. Inaba, “Experimental study of complex mixed-mode oscillations generated in a Bonhoeffer-van der Pol oscillator under weak periodic perturbation,” Chaos, 25, 023105, 2015.

[5] V. Petrov, S.K. Scott, K. Schowalter, “Mixed-mode oscillations in chemical systems,” J. Chem. Phys. vol.97, pp.6191–6198, 1992.

[6] K. Shimizu and N. Inaba, “Piecewise-linear Bonhoeffer-van der Pol dynamics explaining mixed-mode oscillation-incrementing bifurcations,” Progress of Theoretical and Experimental Physics, 2016.

[7] T. Q. Truong, T. Tsubone, K. Shimizu, and N. Inaba, “Experimental Study of Mixed-Mode Oscillations in a Four-Segment Piecewise Linear Bonhoeffer-van der Pol Oscillator under Weak Periodic Perturbation,” IEICE Transactions on Fundamentals of Electronics, Communications and Computer Sciences, vol. E100.A, pp. 1522-1531, 2017.

[8] T. Kousaka, Y. Ogura, K. Shimizu, H. Asahara, and N. Inaba, “Analysis of mixed-mode oscillation-incrementing bifurcations generated in a nonautonomous constrained Bonhoeffer–van der Pol oscillator,” Physica D: Nonlinear Phenomena, vol. 353-354, pp. 48-57, 2017.

[9] A. L. Kawczyński, V. O. Khavrus, and P. E. Strizhak, “Complex mixed-mode periodic and chaotic oscillations in a simple three-variable model of nonlinear system,” Chaos, vol. 10, pp. 299-310, 2000.

[10] N. Matsumiya, K. Shimizu, N. Inaba, “Oscillatory behaviors of axon membrane potential using multi-compartment model of Bonhoeffer-Van der Pol oscillator,” Int. Symp. on Nonlinear Theory and its Applications, pp.483–486, 2022.

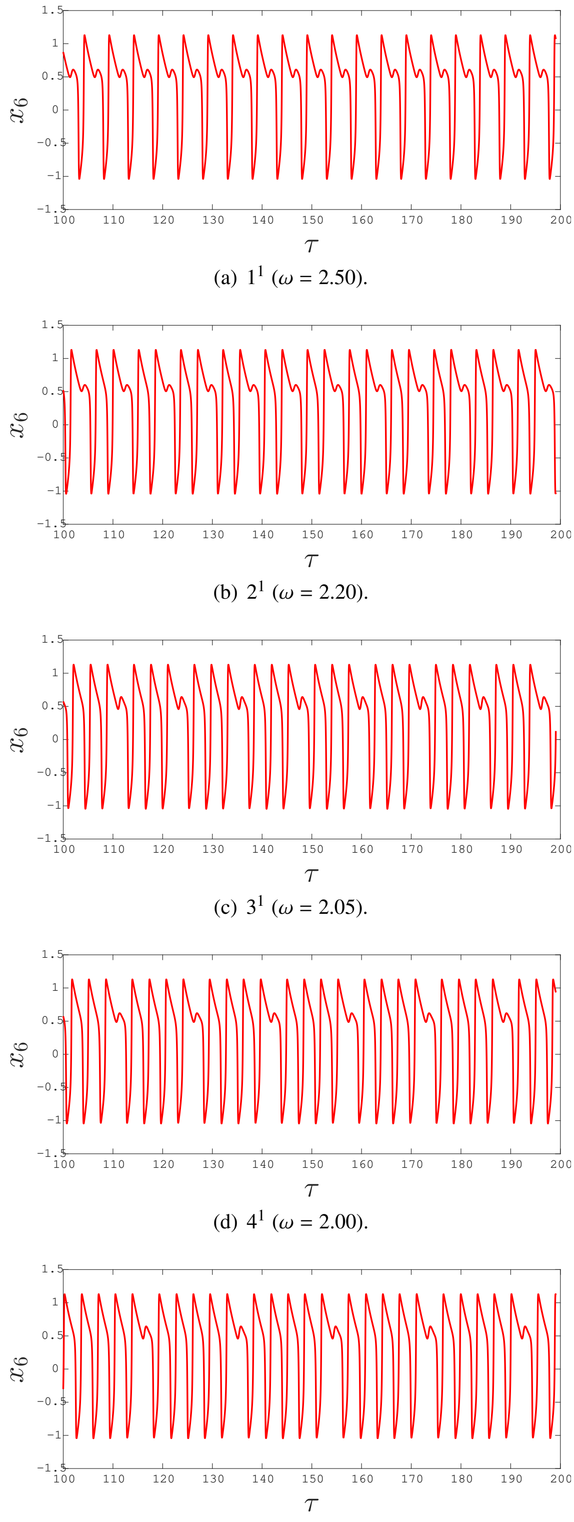

(a) 1^1 ($\omega = 2.50$).

(b) 2^1 ($\omega = 2.20$).

(c) 3^1 ($\omega = 2.05$).

(d) 4^1 ($\omega = 2.00$).

(e) 5^1 ($\omega = 1.96$).

Figure 3: Time series of x_6 for the five distinctive values of ω.

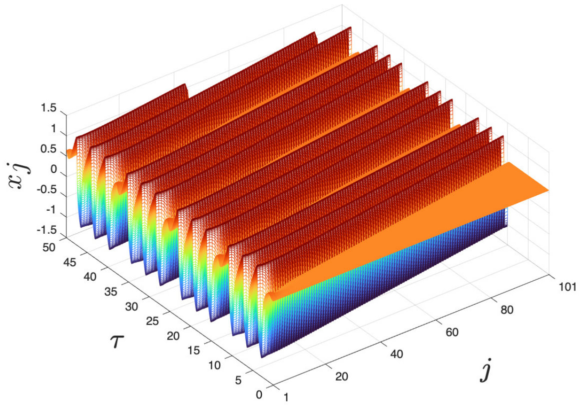

Figure 4: 3D plot of the time series for $\omega = 2.05$.

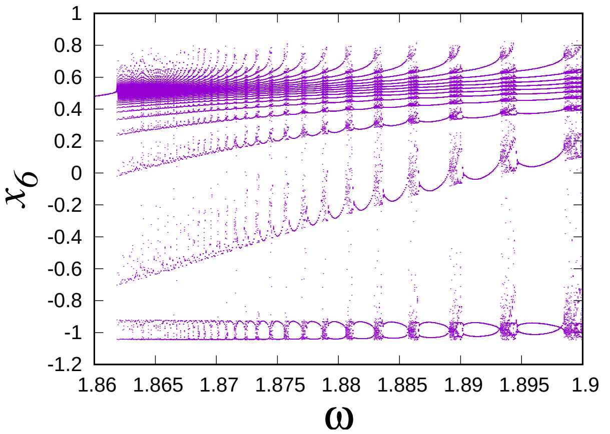

(a) $1.86 \leq \omega \leq 1.9$.

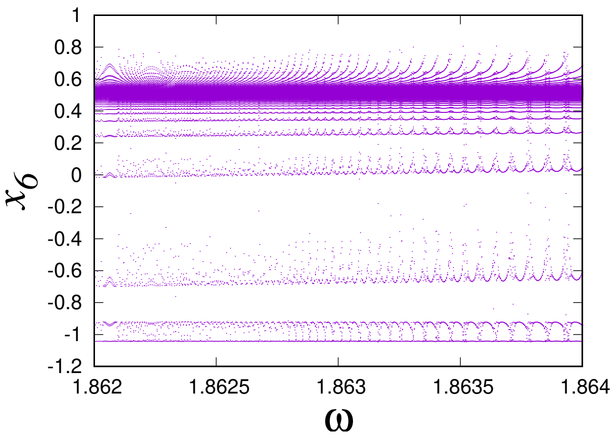

(b) $1.862 \leq \omega \leq 1.864$.

Figure 5: Magnified view of Fig. 2.

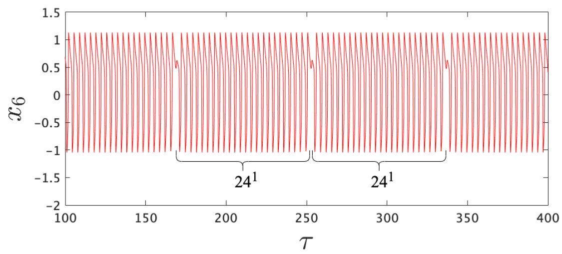

Figure 6: Time series of x_6 for $\omega = 1.87$ (24^1).